Integrity analysis of CO_2 storage sites concerning geochemical-geomechanical interactions in saline aquifers

Arshad Raza[1], Raoof Gholami[1], Mohammad Sarmadivaleh[2], Nathan Tarom[2], Reza Rezaee[2], Chua Han Bing[3], Ramasamy Nagarajan[4], Mohamed Ali Hamid[1], Henry Elochukwu[1]

1-Department of Petroleum Engineering, Curtin University, Malaysia
E-Mail: Arshadraza212@gmail.com
2-Department of Petroleum Engineering, Curtin University, Australia
3-Department of Chemical Engineering, Curtin University, Malaysia.
4-Department of Applied Geology, Curtin University, Malaysia

Abstract

A systematic and careful analysis of changes in the magnitude of geomechanical parameters is essential to mitigate the risk of leakage from CO_2 storage sites. However, depending on rocks and storage sites, these changes might be different due to chemical reactions taking place, especially when it comes to saline aquifers. There have only been few studies carried out in the past to evaluate the maximum sustained pressure of rocks being exposed to these chemical interactions. However, more studies are still required to evaluate the strength of the storage medium or seals when different kinds of rocks and fluids (fresh water or brine) are included in the hostile environment of a storage site. In this paper, attempts were made to evaluate changes in the variation of geomechanical parameters of the Berea sandstone during and after the injection of supercritical CO_2 in a short period of time. The results obtained indicated that the presence of brine in the pore space during injection enhances the severity of geochemical reactions, causing reductions in the magnitudes of elastic parameters including shear modulus. Having a good look into the SEM images of the sample before and after exposure to $scCO_2$ indicated that these changes can be attributed to the dissolution/fracturing of calcite and clays in the matrix of the sample. Although findings were provided based on the pulse measurements tests, more studies are required to have a deeper understanding as to how geochemical reactions may cause difficulties during and after injection into a storage site.

Keyword: CO_2 storage, geomechanics, geochemical interactions, pressure buildup, reservoir integrity

1. Introduction

Carbon capture and storage (CCS) technology has attracted a lot of attention in recent years due to its impact on the reduction of greenhouse gases released into the atmosphere (Bachu et al. 1994; Hitchon, 1996; Ghanbari et al. 2006). Saline aquifers are among the largest storage sites for CO_2 sequestration, although their integrity and technical feasibility require more

[1] Corresponding author Tel: +60105061628
Fax: +6085443837

studies (Raza et al., 2015b; Raza et al. 2016). A saline aquifer is usually composed of sandstone or carbonates and located at the depth of greater than 800 m. They offer natural immobilization of CO_2 due to having favourable chemistry, porosity and subsurface conditions (Riaz and Cinar, 2014).

When CO_2 is injected in this kind of medium, it appears under supercritical conditions due to the pressure and temperature of the site. Storage can then take place through physical trappings (e.g., structural trapping underneath a cap rock, or capillary trapping in the reservoir by interfacial forces) and chemical trappings (e.g., solubility trapping through the dissolution of CO_2 into water, or mineral trapping by chemical interactions of dissolved CO_2 with rocks) (Espinoza et al., 2011; Metz et al., 2005). To achieve a desired mass of CO_2 at the storage site, one should assure that the injection pressure would not exceed the formation fracture pressure which may causes irreversible geomechanical changes in the storage medium or caprock (Rutqvist et al., 2007). This pressure buildup may raise the risk of leakage if the ultimate strength of the seal is exceeded (Dempsey et al., 2014; Espinoza et al., 2011). Therefore, a safe and accurate injection pressure is needed to avoid these changes (Dempsey et al., 2014). This estimation, however, should consider the time-dependant interaction of supercritical (sc) CO_2 with the host medium, which may have a significant impact on geomechanical parameters of reservoirs (Noiriel et al., 2013).

To date, there have been only few attempts to evaluate the effects of CO_2/brine/rock chemical interactions on rock properties, which can help to understand the mechanical response of saline aquifers to injection under different stress states. The aim of this paper is, therefore, to provide an insight into geomechanical changes induced due to geochemical reactions within saline aquifers in a short period of time, which may bring fluctuation in the maximum injection pressure of the storage site.

1.1. Geomechanical effects related to CO_2 injection

1.1.1. Stress Changes

The state of stress in the reservoir is a function of changes in the pore pressure during production or injection phases (Cook et al., 2007). During injection, the reservoir pressure buildup changes the state of in-situ stresses (Alonso et al., 2012; Chiaramonte et al., 2011; Kim and Hosseini, 2014; Rutqvist et al., 2008), causing an increase in the bulk volume, pore compressibility, pore volume and storage capacity (Vulin et al., 2012). These stresses, especially the magnitudes of maximum and minimum horizontal stresses govern the leakage pressure from the reservoir (Lynch et al., 2013; Rutqvist et al., 2008) and vary significantly in a gas storage operation (Cook et al., 2007). In fact, if the pressure increases during injection, the normal stress (which is a combination of in-situ stresses applied perpendicular to the surface of a fault) reduces, causing reactivation of faults or creation of new fractures within the caprock (Ashraf, 2014; Olden et al., 2012; Rutqvist et al., 2007; Varre et al., 2015), depending on the

characteristics of the storage medium and the in-situ stress regime of the field (Olden et al., 2012). Raza et al. (2015b) did a study on the effective parameters of injectivity and concluded that the effect of injection on the in-situ stress must be taken into consideration to have a good estimation of the fracture initiation pressure. In fact, generation of fractures in the caprock may cause difficulty in maintaining the integrity, controlling the capacity, injectivity, and containment of any storage media (Hermanrud et al., 2013; Lynch et al., 2013). This situation can be far worse in saline aquifers due to the absence of fluid productions in closed or semi-closed formations. Active CO_2 Reservoir Management (ACRM) has suggested a brine combined production with injection to enhance the trapping mechanism because CO_2 is more exposed to the storage formation than the seal (Buscheck et al. 2012; Le Guenan and Rohmer, 2011). However, there are many geomechanical issues, which can take place because of pressure buildup in depleted hydrocarbon reservoirs and aquifers which may not be totally eliminated by a combined production. These geomechanical issues have been covered in numerous studies by (i) predictions of the vertical uplift due to the increase in pore pressure (Ferronato et al., 2010; Karimnezhad et al., 2014; Shi and Durucan, 2009; Shi et al., 2013; Tillner et al., 2014; Zhang et al., 2015; Zhu et al., 2015); (ii) modelling of fault reactivations due to injection (Ferronato et al., 2010; Kim and Hosseini, 2014; Olden et al., 2012; Rutqvist et al., 2007; Tillner et al., 2014; Vidal-Gilbert et al., 2010; Zhang et al., 2015); and (iii) analysis of fractures generation within the reservoir and caprock (Alonso et al., 2012; Chiaramonte et al., 2011; Ferronato et al., 2010; Goodarzi et al., 2011; Kim and Hosseini, 2014; Lynch et al., 2013; Rutqvist et al., 2008; Shi and Durucan, 2009). For instance, Rutqvist et al. (2007) proposed a fully coupled numerical analysis to estimate the maximum sustainable injection pressure for the slip tendency of faults in a two-phase system considering continuum stress–strain and discrete fault assessments. The results were compared to a more conventional analytical approach which could only consider a simple reservoir geometry. They concluded that the maximum sustainable injection pressure obtained from the simplified analytical analysis might be uncertain due to neglecting important geometrical factors associated with the injection pressure and stress. Shi and Durucan (2009) carried out a coupled reservoir-geomechanical modelling at the Aztbach-Schwanenstadt gas field for evaluation of the hydro-mechanical response of the reservoir rocks and potential of shear failure and/or re-activation of pre-existing faults considering depletion and injection scenarios. The simulation results showed that compaction and uplifting during production would be experienced under a reversible stress path if the injection pressure exceeds the reservoir initial pressure. They proposed an analytical approach to estimate the sustainable injection pressure by considering the effect of the in-situ stress and rock mechanical properties under the strike-slip faulting regime. Oruganti et al. (2011) presented an analytical model for estimating the pressure profile as a function of time under the constant and infinite acting boundaries of aquifers to mitigate the risk of fracturing, fault reactivation and leakage from abandoned wells. They indicated that Contour of OverPressure (COP) is a function of relative

permeability together with rock properties and it is time-invariant in a constant pressure boundary. On the other hand, when it comes to the infinite-acting boundary condition, COP can be correlated with the rate of change in the aquifer boundary pressure. Goodarzi et. (2011) carried out a geomechanical assessment coupled with a flow model for the feasibility analysis of the Nisku aquifer at the Wabamun Area CO_2 Sequestration project (WASP). The results indicated that injection above the injection pressure increases the potential of well injectivity but enhances the possibility of fracturing the caprock. They concluded that thermal effects due to cold CO_2 injection reduce the fracture pressure and increase the horizontal fracture propagation through caprock. Szulczewski et al. (2011) adopted an effective stress principle to govern the pressure, which would cause tensile fractures in the caprock. According to them, the pressure buildup fractures the rock if the pressure becomes equal to the least principal stress. Lynch et al (2013) examined the stress path hysteresis in a depleted field through a geomechanical-fluid flow modelling for the maximum injection pressure, and concluded that the stress path hysteresis changes during depletion and injection. Kim and Hosseini (2014) presented an analytical approach to estimate the maximum injection pressure to avoid activation of pre-existing fractures in the normal, reverse, and strike-slip faulting regimes. They concluded that the maximum pressure for normal and reverse regimes depends on the horizontal to vertical stress ratio, Poisson's ratio and the saturated rock density.

However, there are some other risks linked to chemical interactions in a brine-saturated medium, which may raise concerns during injection. Table 1 summarizes studies carried out in recent years evaluating the geomechanical aspects of depleted reservoirs and saline aquifers chosen for storage purposes.

1.2 Clastic Reservoirs

CO_2 injection in subsurface geologic media results in changes in poro-elastic responses (Alonso et al., 2012; Chiaramonte et al., 2011; Kim and Hosseini, 2014; Rutqvist et al., 2008). Moreover, chemical interactions during and after injections may change porosity and permeability of rocks through chemically coupled mechanical mechanisms. This mechanism induces creep due to dissolution reactions (Le Guen et al. 2007), enhanced microcracking (Chester et al., 2007; Hangx et al., 2010) and diffusive mass transfer processes (Dewers and Hajash, 1995; Renard et al., 1999), leading to a time-dependent reservoir deformation. Consequently, geomechanical properties, in particular resistance against the pressure build up, may alter as a result of chemical reactions taken place due to development of H_2CO_3 (carbonic acid), HCO_3^- (bicarbonate ions) and CO_3^{2-} (carbonate ions) in the formation saline water (Solomon, 2006; Iglauer et al., 2014). These ions affect the strength of the medium and caprock (Espinoza et al., 2011; Erickson et al., 2015; Varre et al., 2015). Although changes due to chemical reactions are faster in carbonates compared to siliciclastic rocks (Raza et al., 2015b), significant impacts of

these reactions raise a number of concerns when creep can potentially cause reservoirs compactions and damages to wellbores, caprock or fault/seal systems (Hangx et al. 2013).

A detailed review provided by Shukla et al. (2010) on the storage integrity of geologic media highlighted that geomechanical and geochemical properties of reservoirs and caprocks have a significant impact on the outcome of projects. Changes in the stress together with chemical and physical alterations of the reservoir and caprock caused by the carbonic acid (i.e., it is formed by dissolution of CO_2 into ground water), can lead to strength reduction and failure of the caprock (Shukla et al., 2010). Moreover, changes in permeability and porosity of seals may assist the overall penetration of CO_2 into the caprock (Tian et al., 2015).

Numerical and experimental studies carried out in recent years have shown a link between geochemical reactions and geomechanical characteristics of different storage media including sandstone (Dilmore et al., 2008; Doughty, 2010; Zemke et al, 2010; Fischer et al., 2011; Marbler et al. 2012; Hangx et al. 2013; Fischer et al., 2013). For instance, experimental studies performed on sandstone core samples taken from the Utsira reservoir of the Sleipner field, which was saturated with CO_2, revealed that reactions due to having calcite cements take place primarily during the first 8 days with marginal chemical changes (Rochelle, 2002). Hangx et al. (2010) investigated the effects of injection by performing uniaxial compressive tests on quartz sand taken from the Heksenberg formation in the Netherlands. They found that Injection does not induce any remarkable impacts on geomechanical characteristics of sandstone. An experimental study carried out on sandstones samples obtained from different sites (i.e., Otway/Pinjarra and Harvey) for evaluation of the injection pressure before and after CO_2 flooding revealed that the Pinjarra sandstone is not suffering from chemical reactivity while the Harvey-1 plugs did weaken after flooding but changes were not significant (Evans et al., 2012). Hangx et al. (2013) experimentally simulated depletion and injection conditions to study the mechanical properties of sandstone under a representative reservoir condition. They concluded that the chemical interaction of CO_2 causes a complete dissolution of calcite involved in the sandstone composition without any effects on mechanical properties. This is likely due to quartz cements of grains, which is not impacted by CO_2-rich brine. Kempka et al., (2014) did a numerical simulation by considering a time-depended multi-phase flow for evaluation of the mechanical effects of a pilot site from the Ketzin project. They found that the mechanical stability of the caprock, fault and sandstone reservoirs in a long term is maintained with a negligible effect on rock properties. Recently, Varre et al., (2015) numerically studied the influence of geochemical interactions on the geomechanical responses of an aquifer. They concluded that geochemical interactions change the intergranular texture, pore volume, and permeability of rocks. Another experimental study performed by Campos et al., (2015) reported an obvious alteration in the pore system of the Utrillas sandstone because of injection within two months. Experimental and geomechanical modelling carried out by Huq et al. (2015) suggested that permeability of formations might change due to calcite and anhydrite

dissolutions, while calcite dissolution is the major buffering process in the system. Erickson et al. (2015) experimentally studied the geochemical and geomechanical effects of injection on Permotriassic sandstones. They observed changes in mineral surfaces and pore fluid compositions, which affect the deformability and compressive strength of rocks. Table 2 presents the summary of works highlighting the influence of geochemical reactions on mechanical characteristics of sandstone. Table 3 highlights some of the studies carried out to understand the reservoir pressure buildup and geomechanical aspects of storage sites by adopting numerical modelling approaches.

As it is summarised in this table, all of the studies were carried out at a particular injection rate until the specific threshold fracture pressure was reached. Considering the impact of geochemical reactions on petrophysical and geomechanical properties of rocks (i.e., reservoirs and caprock), which may change the fracture pressure variations, it is important to have more clear understanding of changes observed in fracture pressure before and during injection.

Table 1: Summary of recent studies carried out on geomechanical aspects of storage sites

Reference	Approach	Medium/ simulation Time	Objective	Conclusions
(Zhang et al., 2015)	Coupled-geomechanical–fluid flow modelling	Aquifer/ 20 year	Fault reactivation Ground surface uplifts	No changes in the farcture pressure by the injection rate of 1–5 million tons per year on faults but ground surface uplifts
(Zhu et al., 2015)	Coupled geomechanical–fluid flow modelling	Aquifer/ 10 years	Reservoir stresses	Maximum ground surface uplift of 1.49 mm!
(Kim and Hosseini, 2014)	Analytical	-	Reactivation of pre-existing fractures	New equations were devloped for determination of maximum pressure for different stress regimes
(Tillner et al., 2014)	Coupled geomechanical–fluid flow modelling	Aquifer/ 40years	-Leakage through fault - Reservoir stresses	A Large area was affected by ground surface uplift. Neither fault slip nor dilation remained unchanged by CO_2 injection
(Shi et al., 2013)	Coupled geomechanical–fluid flow modelling	Aquifer/ 5 year	Reservoir stresses	A low vertical surface uplift, accompanied by an enhanced horizontal displacement
(Olden et al., 2012)	Lab/ geomechanical modelling	Aquifer/ 7000 years	Shear failure of interact rock Fault Reactivation	Models were proposed and initially used to determine generic geomechanical property
(Alonso et al., 2012)	finite element model	Aquifer/ 5.5-22years	Potential leakage path	Injection exceeds the yield strength of rocks causing deformation in brittle regime and generation of flow paths
(Goodarzi et al., 2011)	geomechanical modelling	Aquifer/ 50years	Fracture initiation	The possibility of fracturing caprock increases due to reaching the fracture pressure limits
(Rutqvist et al., 2007)	Coupled-geomechanical–fluid flow modelling	Aquifer/2.5years	fault-slip analysis	A fully coupled numerical analysis was provided to estimate the maximum sustainable pressure by considering the structural geometry, fluid pressure and in-situ stress of the field
(Lynch et al., 2013)	Coupled geomechanical–fluid flow modelling	Scenario of depleted oil & gas/20 years	Stress path hysteresis	Fractures are key controlling parameters to estimate the capacity and injectivity of any storage sites
(Chiaramonte et al., 2011)	stochastic 3D geomechanical modelling	Oil reservoir/6 weeks	Role of minor faults and fault reactivation	No risk of fault reactivation, or losing the caprock integrity by the buoyancy pressure of the maximum CO_2 column height
(Ferronato et al., 2010)	geomechanical modelling	Gas reservoir/ 22-150 years (Uplift) 140 years (stress)	Reservoir stresses Fault reactivation	Reactivation of faults with generation of preferential leakage pathways, and possible local shear or tensile failures in the caprock with land uplift process

(Shi and Durucan, 2009)	Coupled-geomechanical–fluid flow modelling	gas reservoir/40 years	Reservoir stresses	Due to variation in stresses, depletion has resulted in formation compaction while injection causes uplift under strike-slip fault stress regime

Table 2: Summary of studies carried out on geochemical effects of injection on geomechanical parameters

Reference	Approach	Rock/medium	Experiment time	Effect	Conclusions
(Hangx et al., 2010)	Experimental	Sandstone/ Aquifer and Oil	6 days	Yes	No significant impact on mechanical properties
(Zemke et al, 2010)	Experimental	Sandstone/ aquifer	Several months	Minor	A slight increase of porosity
(Fischer et al. 2011)	Experimental	Sandstone/ aquifer	63 days	Minor	Dissolution of calcium-rich plagioclase, K-feldspar and anhydrite, and stabilization or precipitation of albite, together with slight changes in petrophysical properties
(Evans et al., 2012).	Experimental	Sandstones	-	Minor	Minor effect on geomechanical properties of sandstone after CO_2 flood
(Marbler et al. 2012)	Experimental	Sandstones	2-4 weeks	Yes	The exposure to pure $scCO_2$ in the autoclave system induces reduced strength parameters, modified elastic deformation behaviour and changes of the effective porosity in comparison to untreated sandstone.
(Hangx et al., 2013)	Experimental	Sandstones	6 days	No	Calcite-dissolution-induced weakening may have a significant impact on none quartz cemented sandstone
(Kempka et al., 2014).	Numerical modeling	Aquifer/ Sandstones	>50 years	Yes	Mechanical stability of the storage medium is affected by geochemical reactions
(Varre et al., 2015)	Numerical modeling	Sandstones/ Aquifer	25 years - injection 1000 years- monitoring	Minor	Geochemical processes do not have a significant influence on porosity and geomechanical properties of reservoirs
(Campos et al., 2015)	Experimental/ pore network modeling	Sandstone/ Aquifer	2 months	Yes	Modification in the pore system after two months periods of injection
(Hangx et al., 2015)	Experimental	Sandstone/ Depleted oil reservoir	Short term (hours to days)	Minor	Minor effect on the petrophysical and geomechanical properties of sandstone.
(Huq et al., 2015)	Experimental/ Numerical modeling	Sandstone -	6 days	Yes	Predominant dissolution of anhydrite causing an increase in concentrations of calcium and sulfate at early stages of injection. Permeability of sample increases due to dissolution of cement.
(Erickson et al. 2015)	Experimental	Sandstones/ -	Some weeks	Yes	Changes in deformability and compressive strength of rocks due to compositional changes

Table 3: Summary of studies performed on the storage in different geologic mediums

Reference	Storage Medium	Storage capacity	Reservoir Fracture threshold (bar)	Injection Time (years)	Injection Rate	Maximum pressure at the end of injection (bar)	Simulation Time including injection period (years)	Aspect
(Ghanbari et al., 2006)	Aquifer	-	-	30	0.514 MMscf/d	73	500	Sensitivity Analysis of hydrodynamic and solubility trappings
(Ukaegbu et al., 2009)	Aquifer	1.12 BScf	94	2.5	1.2 MMscf/d	86.5	20	Sensitivity analysis of CO_2distribution
(Birkholzer et al., 2011)	Faulted Sandstone Basin	250 Mt	-	50	5 Mt/yr	(a)30 (b) 23	100	Pressure build up and brine migration across the fault or caprock
(Le Guenan and Rohmer, 2011)	Aquifer	10 Mt	39.9	10	1 Mt/yr	42	11	Pressure buildup near well bore and far away region
(Arts et al., 2012)	Depleted gas	8 Mt	-	10	1.5 Mt/yr	350	10	Feasibility study regarding injection rate and pressure buildup
(Buscheck et al., 2012)	Aquifer	114 Mt -	-	30 30-100	3.8 Mt/yr 0.95, 1.9, 3.8, and 7.6 Mt/yr	(a)40 (b)10.8	30 (vertical well case) 30-100 (horizontal well case)	Pressure builds up and injectivity was considered for two scenarios: (a) no brine production, and (b) with brine production
(Wainwright et al., 2013)	Basin/ Aquifer	250 Mt	0.58 (seal)	50	5 Mt/yr	>0.58	200	Pressure build up and CO_2 migration
(Benisch and Bauer, 2013)	North German Basin/two phase	20Mt	-	20	1 Mt/yr	180-60	60-50,000	Pressure builds-up near and far away from the wellbore and caprock integritywas monitored
(Hermanrud et al., 2013)	Gas field	17-25 Gt	390	3	-	390	3	Pressure build up
(Snippe and Tucker, 2014)	Depleted gas & dipping Aquifer	-	-	10	-	200	10,000	Water-rock interactions and trappings
(Mbia et al., 2014)	Aquifer	60Mt	70.2	40	1.5 Mt/yr	54	140	Pressure buildup responses against the variation of caprock compressibility
(Tillner et al., 2014)	Aquifer	80 Mt	-	40	2 Mt/yr	334-371	40	Storage integrity and uplift due to pressure buildup by coupling the dynamic and mechanical simulations
(Hussain et al., 2015)	Aquifer	56.4 Mt	250 (seal)	30	0.94 Mt/yr	20-70	100	Pressure buildup and its effect on ground water

2. Geomechanical-Geochemical interactions

The geomechanical effects of short and long-terms exposure to $scCO_2$ on reservoir rocks have not been fully understood. In this section, attempts were made to evaluate the geochemical reactions taking place in the Berea sandstone after being saturated by $scCO_2$. A series of ultrasonic pulse measurements were performed and dynamic elastic parameters were estimated using the velocity of P- and S-waves recorded. This may help to understand how body waves can be used to evaluate changes in the characteristics of reservoirs and seal rocks while storage is in progress.

2.1. Sample Characterizations

Berea sandstone was used for the purpose of this study to evaluate changes taking place due to the injection of $scCO_2$ into a fully saturated brine sample. A series of petrophysical and image analysis was carried out to understand physical, mineralogical and fabric properties of the sample. The petrophysical tests conducted consisted of: 1) Hg injection porosimetry for pore size distribution estimation, 2) permeability determination using an air permeameter, 3) X-ray diffraction (XRD) analysis and 4) X-ray fluorescence (XRF). The bulk density was measured by determination of the volume of the samples and its dry mass. The saturated density could then be calculated using the sample porosity and the fluid density. The density of the fluid (brine and $scCO_2$) was determined using the NIST Chemistry Web-Book (webbook.nist.gov) under different pressure and temperature conditions.

An imaging analysis using the Scanning Electron Microscope (SEM) was done in different scales to examine the texture and microstructure of the sample before and after exposure to $scCO_2$. Table 4 and 5, respectively, gives the physical properties and distribution of minerals in the sample. Tables 6 summarizes the results obtained from the XRF analysis. Figure 1 and 2, respectively, shows the SEM images and the pore throat size of the sample.

Table 4: Physical properties of the Berea sample used for the purpose of this study

Samples	Density (g/cm^3)	Porosity (V/V)	Permeability (mD)	Young's Modulus (GPa)	Shear Modulus (GPa)	Poisson's ratio	Compressive Strength (MPa)	Tensile Strength (MPa)
B.1	2.3	0.19	420	25.3	10.2	0.25	53	~5

Table 5: Mineral types and distribution in the sample

Samples	Quartz (%)	Microcline (%)	Kaolinte (%)	Chlorite (%)	Albite (%)	Ankerite (%)
B.1	80	6.7	7.3	1.4	2.9	1.7

Table 6: Chemical element included in the structure of the sample

Samples	SiO_2 (%)	Al_2O_3 (%)	Fe_2O_3 (%)	FeO (%)	MgO (%)	CaO (%)	Total (%)
Berea Sandstone	93.13	3.86	0.11	0.54	0.25	0.10	97.99

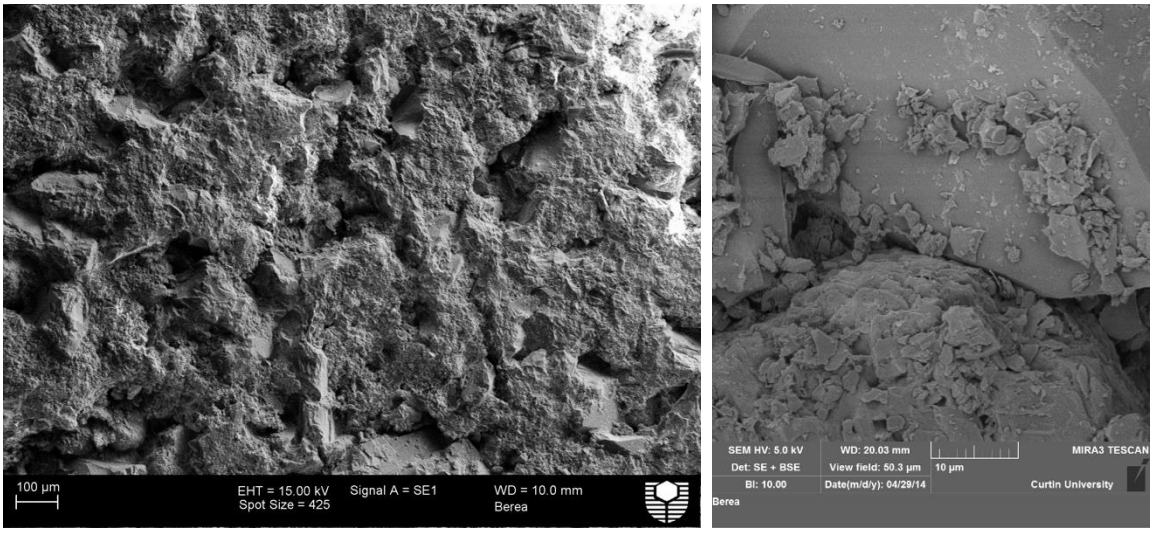

Figure 1: Scanning Electron Microscope (SEM) image of the Berea sandstone. Big grains of quartz and dispersed clays are observed in the sample (right side)

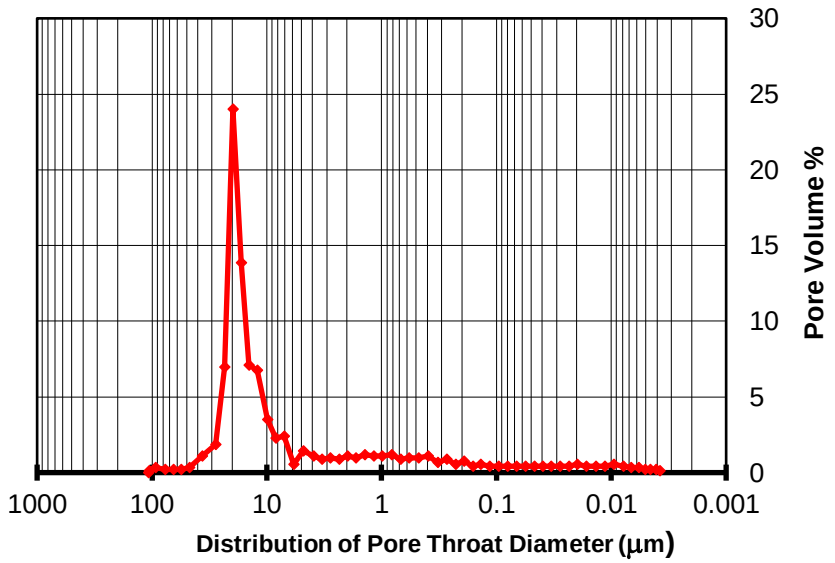

Figure 2: Pore throat size of the sample with an average of 8µm

As it is seen in Table 5, the Berea sandstone composed of quartz, feldspars (microcline), kaolinite, chlorite, albite and ankerite (carbonate) with a high permeability and porosity values. Table 7 summarizes the chemical reactions observed in sandstone reservoirs having the above minerals.

According to Rathnaweera et al., (2016), calcite dissolution is predominant in a short-term scale compared to other reaction mechanisms involved. The reaction rate on these occasions are directly related to the CO_2 partial pressure and indirectly attributed to the pore fluid pH, and temperature (Rathnaweera et al., 2016). In the case of siliclastic sandstones, quartz doesn't make a significant contribution into the geochemical reactions and it is often part of as a long-

term reaction dominated by the mineral trapping process (De Silva et al., 2015). Aluminosilicates Including feldspars, micas, and clays have a slow rate of reaction but it is not as much slow as that of quartz. Feldspars and clay minerals such as anorthite, illite and kaolinite tend to dissolve in a low pH environment created due to generation of the carbonic acid (De Silva et al., 2015). During the dissolution of kaolinite, for instance, the rock mass pore structure is affected by changes of grain-to-grain contacts (Rathnaweera et al., 2016). Considering these rate of reactions for the minerals included in the Berea sandstone, it seems that the dissolution of calcite and dolomite might be the fastest mechanism taking place during and after CO_2 injection in a short-term scale causing geomechanical changes, followed by a slower chemical reaction of aluminosilicats (feldspars and clays).

Table 7: Mineral-CO_2-brine interactions taking place in sandstone reservoirs ([1]Espinoza et al., 2011; [2]De Silva et al., 2015)

Primary mineral	Reaction	Reaction Rate[(1)]	Secondary mineral
Dissolution Reactions			
	$CO_2(g) \rightarrow CO_2(aq)$ $CO_2(g) + H_2O(l) \rightleftharpoons H_2CO_3(aq)$ $H_2CO_3(aq) \rightleftharpoons H^+(aq) + HCO_3^-(aq)$ $HCO_3^-(aq) \rightleftharpoons H^+(aq) + CO_3^{2-}(aq)$		
Silicates[(1)]	$SiO_{2(s)} + 2H_2O \rightleftharpoons H_4SiO_4 \rightleftharpoons H^+ + H_3SiO_4^- \rightleftharpoons H^+ + H_2SiO_4^{2-}$	1.26×10^{-14} mol.m^{-2}s^{-1}	Solubility of quartz does not change with concentration of dissolved CO_2.
Kaolinite[(2)]	$Al_2Si_2O_5(OH)_4(s) + 6H^+(aq) \rightarrow 5H_2O + 2SiO_2(aq) + 2Al^{3+}(aq)$	10^{-14}-to-10^{-15} mol.m^{-2}s^{-1}	Complete Dissolution
Arnorthite[(2)]	$CaAl_2Si_2O_8(s) + CO_2(g) + 2H_2O(l) \rightarrow CaCO_3(s) + Al_2Si_2O_5(OH)_4(s)$	1.2×10^{-5} mol.m^{-2}s^{-1}	Calcite, kaolinite
Illite[(2)]	$Illite + 8H^+(aq) \Longrightarrow 5H_2O(l) + 0.6K^+(aq) + 0.25Mg^{2+}(aq) + 3.5SiO_2(aq) + 2.3Al^{3+}(aq)$	-	Complete Dissolution
Labradorite[(2)]	$Ca_{0.6}Na_{0.4}Al_{1.6}Si_{2.4}O_8 + 5.4H^+(aq) + CO_2(aq) \rightarrow 0.6Ca^{2+}(aq) + HCO_3^-(aq) + 2.2H_2O(l) + 0.4Na^+(aq) + 1.6Al^{3+} + 2.4SiO_2(aq)$	-	Complete Dissolution
Albite[(2)]	$NaAlSi_3O_8(s) + CO_2(g) + H_2O(l) \rightarrow NaAl(CO_3)(OH)_2(s) + 3SiO_2(s)$	-	Dawsonite, quartz
K-feldspar[(2)]	$KAlSi_3O_8(s) + Na^+(aq) + CO_2(g) + 2H_2O(l) \rightarrow NaAl(CO_3)(OH)_2(s) + 3SiO_2(s) + K^+(aq)$	-	Dawsonite, quartz
Calcite[(2)]	$CaCO_3(s) + H^+(aq) \rightarrow Ca^{2+}(aq) + HCO_3^-(aq)$, *at high PH values only*	1.6-to-3.2×10^{-5} mol.m^{-2}s^{-1}	Complete Dissolution
Glauconite[(2)]	$Glauconite + 14H^+(aq) \Longrightarrow 1.5K^+(aq) + 2.5Fe^{3+}(aq) + 0.5Fe^{2+}(aq) + Mg^{2+}(aq) + 1.0Al^{3+}(aq) + 7.5SiO_2(aq) + 9H_2O(l)$		Quartz
Annite[(2)]	$annite + 3CO_2 \rightleftharpoons 3siderite + K\text{-feldspar}$		Siderite, K-feldspar
Chlorite[(2)]	$Chlorite + 20H^+(aq) \Longrightarrow 5Fe^{2+}(aq) + 5Mg^{2+}(aq) + 4Al(OH)_3(aq) + 6H_4SiO_4(aq)$		Aluminium hydroxide
Dolomite[(2)]	$CaMg(CO_3)_2(s) + 2H^+(aq) + Mg^{2+}(aq) + HCO_3^-(aq)$		Complete Dissolution
Precipitation Reactions[(2)]			
	$Ca^{2+}(aq) + CO_3^{2-}(aq) \rightarrow CaCO_3(s)$		Calcite
	$Fe^{2+}(aq) + CO_3^{2-}(aq) \rightarrow FeCO_3(s)$		Siderite
	$Mg^{2+}(aq) + CO_3^{2-}(aq) \rightarrow MgCO_3(s)$		Magnesite
	$Ca^{2+}(aq) + SO_4^{2-}(aq) \rightarrow CaSO_4(s)$		Anhydrite
	$K^+(aq) + 3Al^{3+}(aq) + 2SO_4^{2-}(aq) + 6H_2O(l) \rightarrow KAl_3(SO_4)_2(OH)_6(s) + 6H^+(aq)$		Alunite
	$Ca^{2+}(aq) + Mg^{2+}(aq) + 2HCO_3^-(aq) \rightarrow CaMg(CO_3)_2(s) + 2H^+(aq)$		Dolomite

2.2. Ultrasonic Pulse Measurement

The ultrasonic pulse measurement system setup used in this study is available in the department of Petroleum Engineering at Curtin University, Australia. The experimental setup consists of a pulse generator unit, transducers, a signal conditioner, and a computer equipped with a high frequency analog to digital (A/D) converter. Measurement were conducted using a triaxial (Hoek) high pressure cell, which allows axial loading of up to 150 MPa, with a confining

and pore pressure of 40 MPa and 20 MPa respectively while temperature could be varied from ambient conditions to up to 80°C. Piezoelectric crystals were used for the pulse transmission and converting electric signals into mechanical vibrations modes of compressional (P) and shear (S). Figure 3 shows the location of the Berea sample in the triaxial cell used for the pulse measurements.

To accurately measure S-wave velocity which is often tricky to record in traditional experimental setups, due to placing transducers very close to samples, transducers were separated from the sample by 60-mm-long plastic cylinders. This set up decreases wave reverberations inside platens and prevents contamination of the S-wave arrival time because of the proximity of acoustic impedances of the plastic cylinder in the rock sample. Calibration of the system was performed over the whole range of pressures and temperatures using aluminum and stainless steel samples with the same lengths and diameters as that of the sample. Ultrasonic compressional and shear wave velocities along the symmetry axis of the sample were then measured with a nominal pulse central frequency of 0.5 MHz.

To decrease the random noise, the recorded waveforms were a stack of 100 traces. The experimental errors in determination of P- and S-wave velocities were respectively 1% and 1.5%, induced mainly because of the uncertainty in picking up the arrival time of the waves recorded.

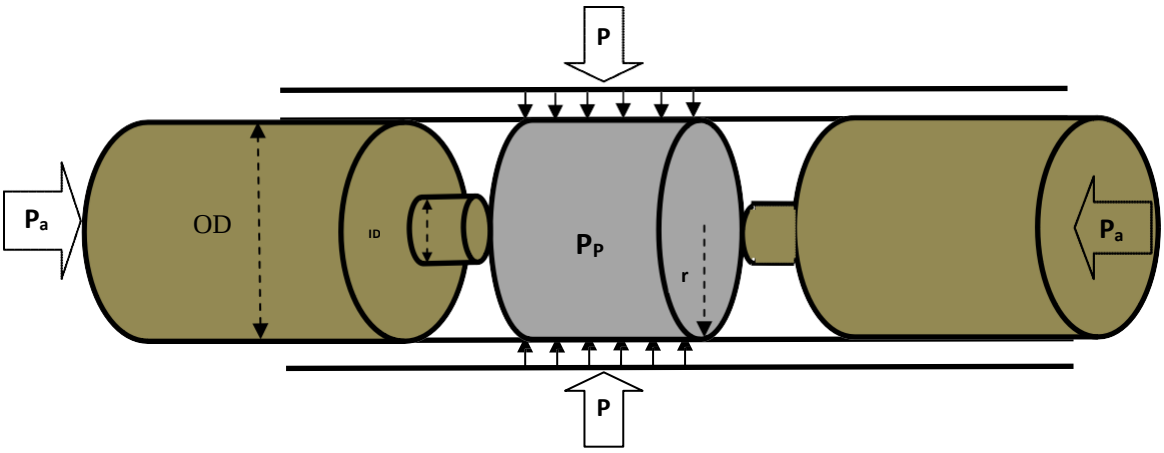

Figure 3: Location of the sample between transducers under the confining pressure (P), axial stress (Pa) and pore pressure (Pp)

It should be noticed that the following nomenclature was used in this study to describe the lab protocol:

i. Confining pressure (Pc): The external (pressure) stress applied to the sample;
ii. Pore pressure (Pp): The internal pressure of the fluid (brine and $scCO_2$) occupying the pore space of the sample;
iii. Differential pressure (Pd): the difference between the confining and pore pressures.

2.3. Saturation Control

When injection in an aquifer begins, CO_2 dissolves into the brine, which reduces the pH of the system and increases mineral dissolutions and precipitations. This acidification is followed by desiccation in which CO_2 gas bubbles are created around the injection well, pushing the formation water away from the injection site. This leads to formation of a dry zone with a gas saturation degree of almost 1. This dry zone is surrounded by a mixed zone partially saturated by brine and free $scCO_2$. In the more remote parts of the aquifer, however, an aqueous phase fully saturated by brine exist which will be further pushed as injection progresses (Rathnaweera et al., 2015). To simulate this condition, the sandstone sample was gone through the pulse measurement under the following three different conditions:

- **Dry Sample:** The sample was subjected to the ultrasound cleaning in distilled water and then placed in an oven at 105 °C for 24 hours. The dry mass of the specimen was measured after cooling to the room temperature followed by the pulse measurements to record P- and S-waves transit times at different confining pressures ranging from 1 to 30 MPa.
- **Brine Saturated Sample:** A brine solution with the salinity of 1500 ppm containing 5 wt% NaCl and 1 wt% KCl was prepared at this stage. Saturation was initiated by injecting brine into the sample for almost one hour to release all of the gases. Upon full saturation, the outlet valve was closed and the pore pressure was increased to 1.5 MPa. This was followed by conducting the ultrasonic tests under different confining pressures ranging from 0 to ~21MPa while the maximum pore pressure observed was 18MPa. Figure 4 shows two of the waveforms obtained from these measurements under the pore and confining pressures of 15 MPa.
- **CO_2 Saturated Sample:** Carbon dioxide in the supercritical phase ($scCO_2$) was injected using the syringe pump into the brine saturated sample. Syringe pump, tubes, and high-pressure cell were heated and maintained at a temperature of 35°C while the confining pressure was varied from 10MPa to ~24MPa to have a fully $scCO_2$ saturated sample. The volume flow rate of $scCO_2$ injected was carefully observed through injection and the volume of brine collected from the sample was used to estimate the average saturation of CO_2 in the sample. Gnerally, the sample was exposed to $scCO_2$ for five days. Figure 5 shows two of the waveforms obtained from these measurements under the pore pressure of 14 MPa and confining pressure of 20 MPa.

2.4. Injection Pressure and Magnitude of Stress

Amplitude is one of the important parameters, carrying a lot of information related to the wave behaviour and its attenuation (Alemu et al. 2013). It would, therefore, be a very useful attribute which can be used for characterizations of rocks while being saturated with different kinds of fluids. In this section, attempts were made to evaluate the effect of injection (increases in the

pore pressure) and in-situ stress (confining pressure) on the acoustic response of the sample when it is saturated with brine and flooded by $scCO_2$. This helps to understand the possible changes taking place in the elastic and strength parameters of aquifers during and after injection.

As mentioned earlier, the pulse measurement was done at different confining pressures on the dry sample. Figure 6 shows the quality of the P-wave amplitude received under three different confining pressures.

From this Figure, one may conclude that as the confining pressure increases, the amplitude increases and attenuation decreases under a dry condition. This could be due to the reduction in the matrix anelasticity and closure of pores and cracks in the sample matrix (Thakur and Rajput, 2010). Such stress dependency is typical for sandstones and can be explained theoretically with the dual-porosity model (Shapiro, 2003; Pervukhina et al., 2010).

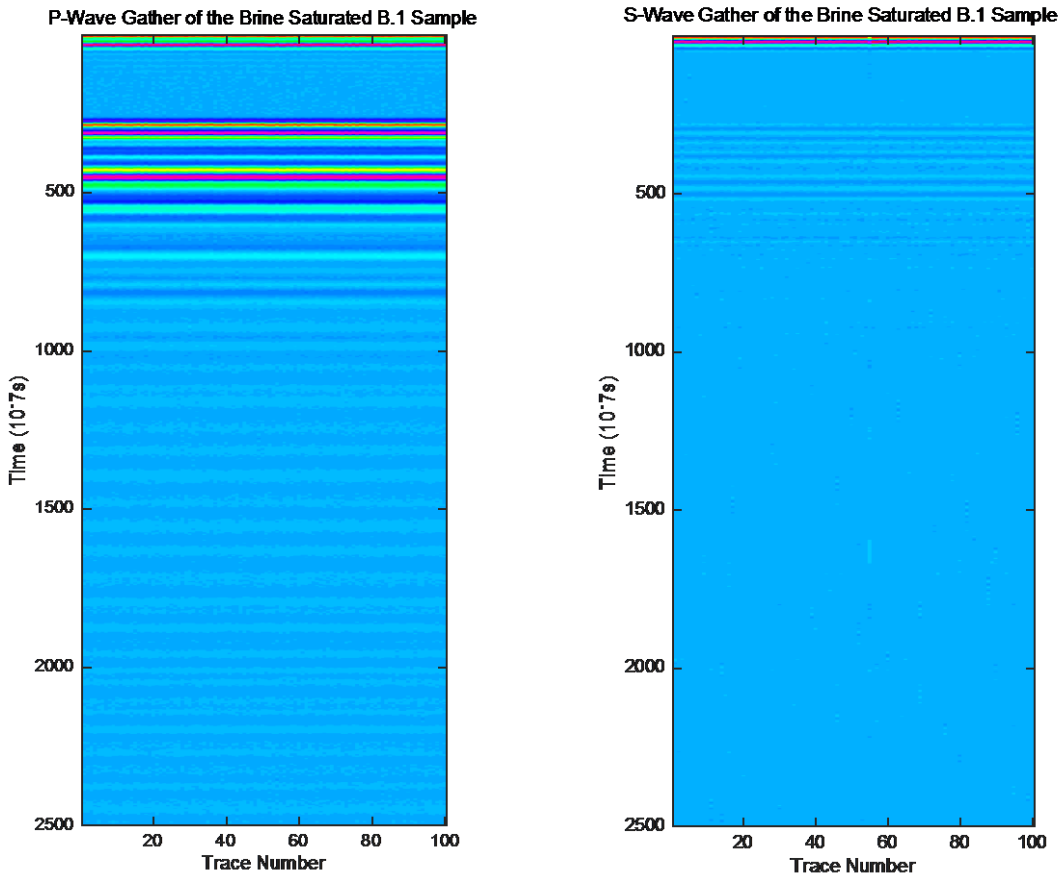

Figure 4: P-wave (left) and S-wave (right) waveforms obtained from the pulse measurements on the brine saturated sample under the pore and confining pressure of 15 MPa. Colours are amplitude variations

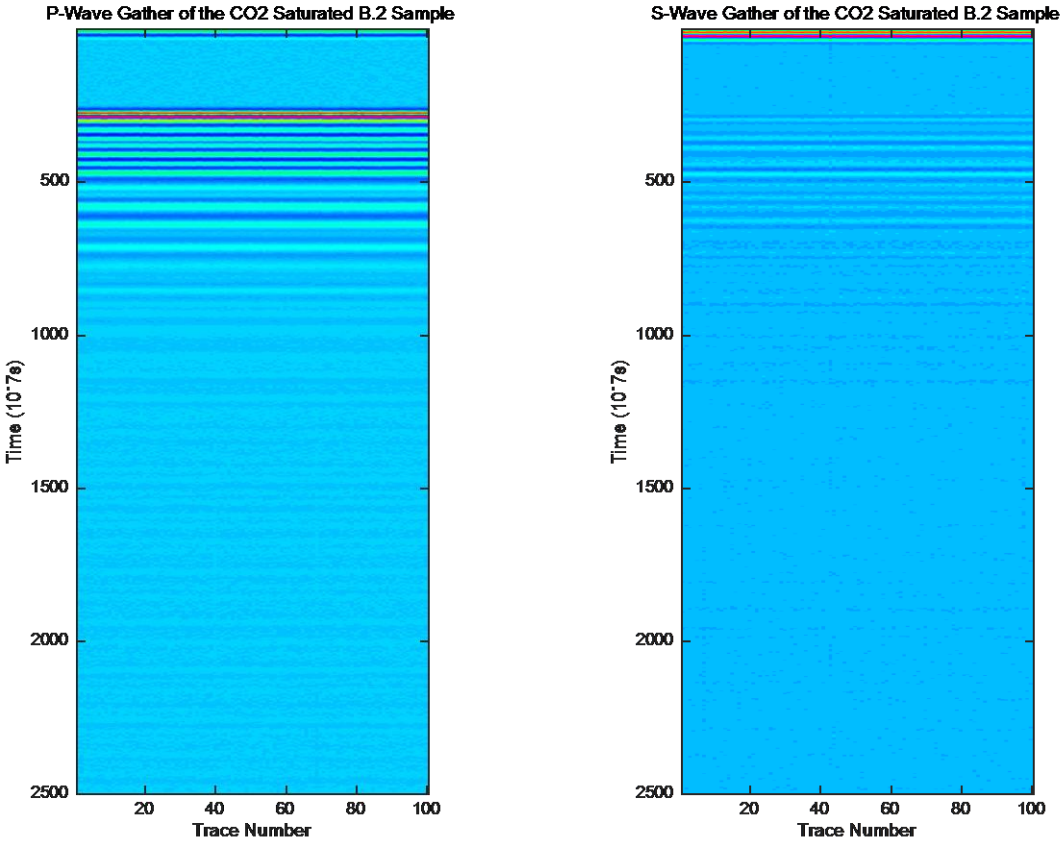

Figure 5: P-wave (left) and S-wave (right) waveforms obtained from the pulse measurements on the $scCO_2$ saturated sample under the pore pressure of 14 MPa and confining pressure of 20 MPa. Colours are amplitude variations

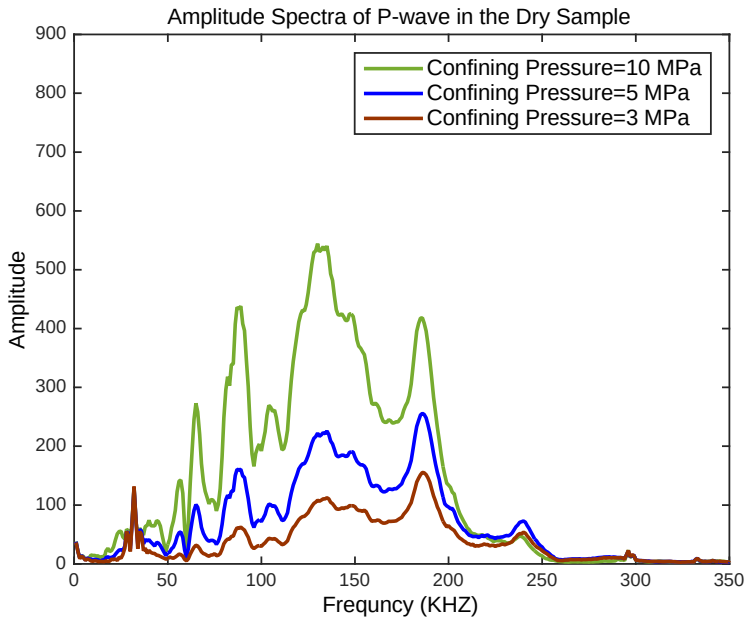

Figure 6: Amplitude spectra of P-wave obtained from the tests on the dry sample

The results obtained from the pulse measurement on the brine saturated sample, in the next stage, indicated that as the confining pressure increases, the amplitude increases due to the closure of the penny shaped pores and thin cracks as well as the compaction of the grains and cement in the sample (Njiekak et al. 2013) (See Figure 7). It was also found that increasing the confining pressure increases the density and bulk modulus of the samples because of the compaction effect. This increases in the bulk modulus was more pronounced than the density as the attenuation of the compressional wave was reduced in the brine saturated samples under a high confining pressure.

In contrast, the pore pressure revealed that in a same confining pressure, any increases in the pore pressure decreases the amplitude of P-wave going through the brine saturated sample (See Figure 8). This is mainly because the pore pressure opens the pores and increases the overall density (Chen et al., 2013). It was then concluded that as the in-situ stress decreases due to the pore pressure increase, stiffness and strength of the medium chosen as the storage site reduces remarkably.

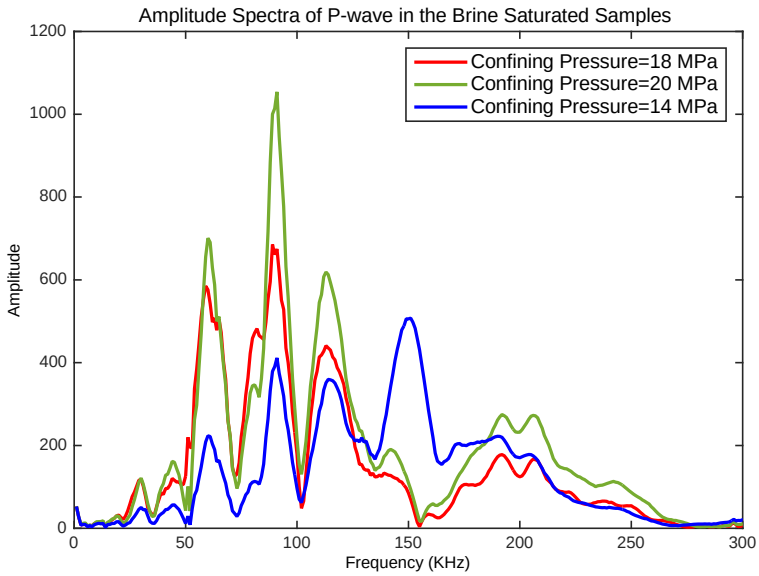

Figure 7: Amplitude spectra of P-wave at as a function of the confining pressure at the pore pressure of 14 MPa in the brine saturated sample

In the next step, the effect of the pore and confining pressure on the acoustic response of the samples being flooded by $scCO_2$ were evaluated. The results obtained indicated that regardless of the confining pressure, the amplitude of P-wave would generally decrease as brine is replaced by CO_2 in the pore spaces. This decreases in the amplitude can be attributed to the reduction of the bulk modulus of the fluids as well as the distribution, extrusion, and movement of $scCO_2$ in the pore space of the sample. Compression and expansion of cracks and pore spaces can be another reason of attenuation which should not be neglected (Njiekak et al. 2013). As a result, the amplitude of the P-wave initially decreases as the injection of $scCO_2$ begins and then rises as the saturation progresses. This amplitude variation and reduction might be a good sign of detecting CO_2 at the early stage of injection in an aquifer.

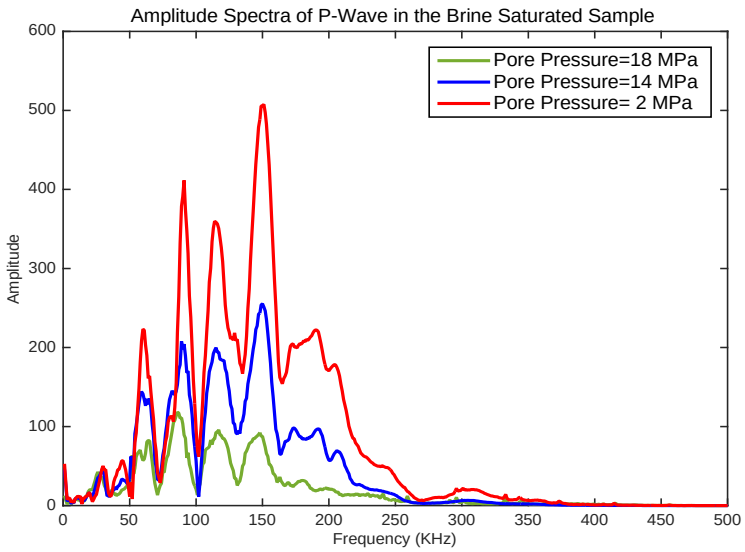

Figure 8: Amplitude spectra of P-wave as a function of the pore pressure in the brine saturated sample under a same confining pressure of 20 MPa

Another observation made during $scCO_2$ injection revealed that as the pore pressure increases, or the confining pressure decreases, the amplitude dispersion increases but this dispersion was more pronounced than that of the brine saturated sample which could be related to the physical properties of CO_2. Figure 9 and 10 show the amplitude of P-wave obtained during $scCO_2$ injection.

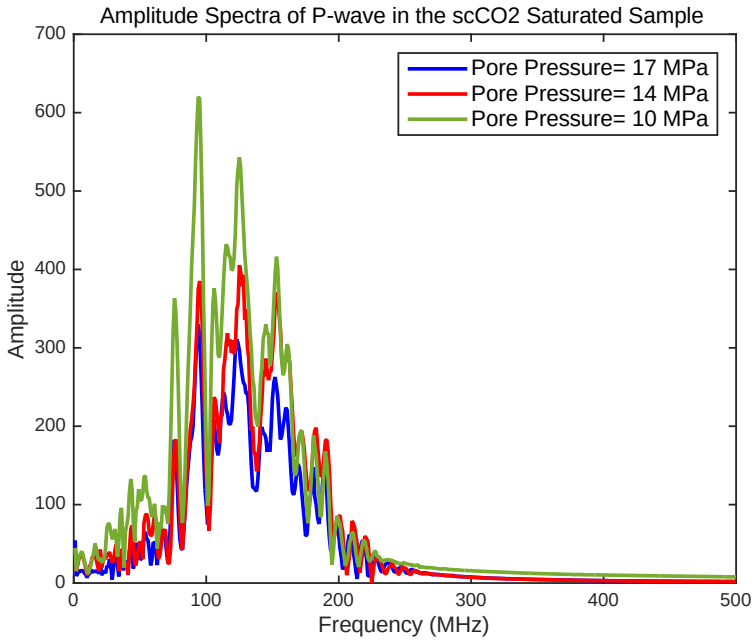

Figure 9: Amplitude spectra of P-wave as a function of the pore pressure during $scCO_2$ injection under the confining pressure of 20 MPa

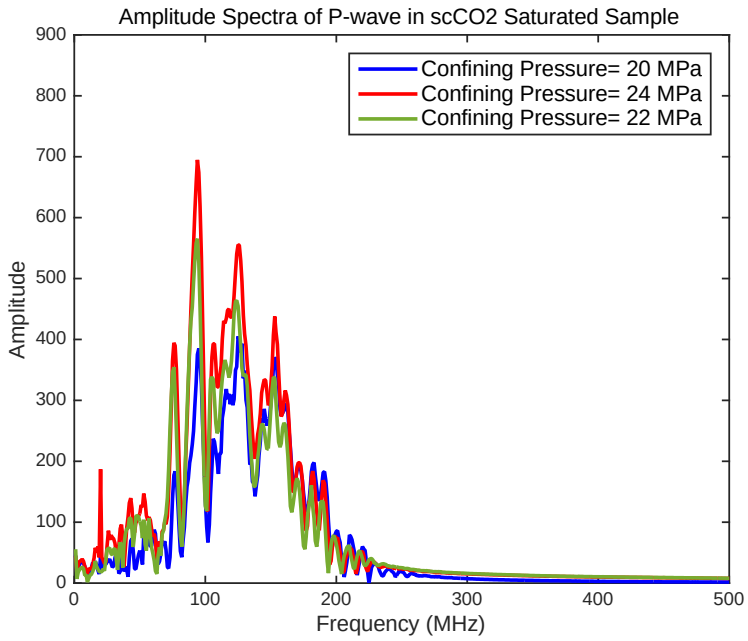

Figure 10: Amplitude spectra of P-wave as a function of the confining pressures during $scCO_2$ injection under the pore pressure of 14 MPa

2.5. Elastic Parameters

In order to have a good insight into the changes taking place due to the fluid substitution in the sample using the wave velocity, it was crucial to ensure that any variations in the waveform is due to changes in the pore fluid physical properties and alterations of the sample's solid framework. Thus, a constant differential pressure of 3 MPa was upheld at different stages by assuming that the increase in the confining pressure can cancel the effect of the pore pressure. Figure 11 shows the velocity of P- and S-waves obtained from the sample saturated by brine and flooded by $scCO_2$ under the differential pressure of 3 MPa.

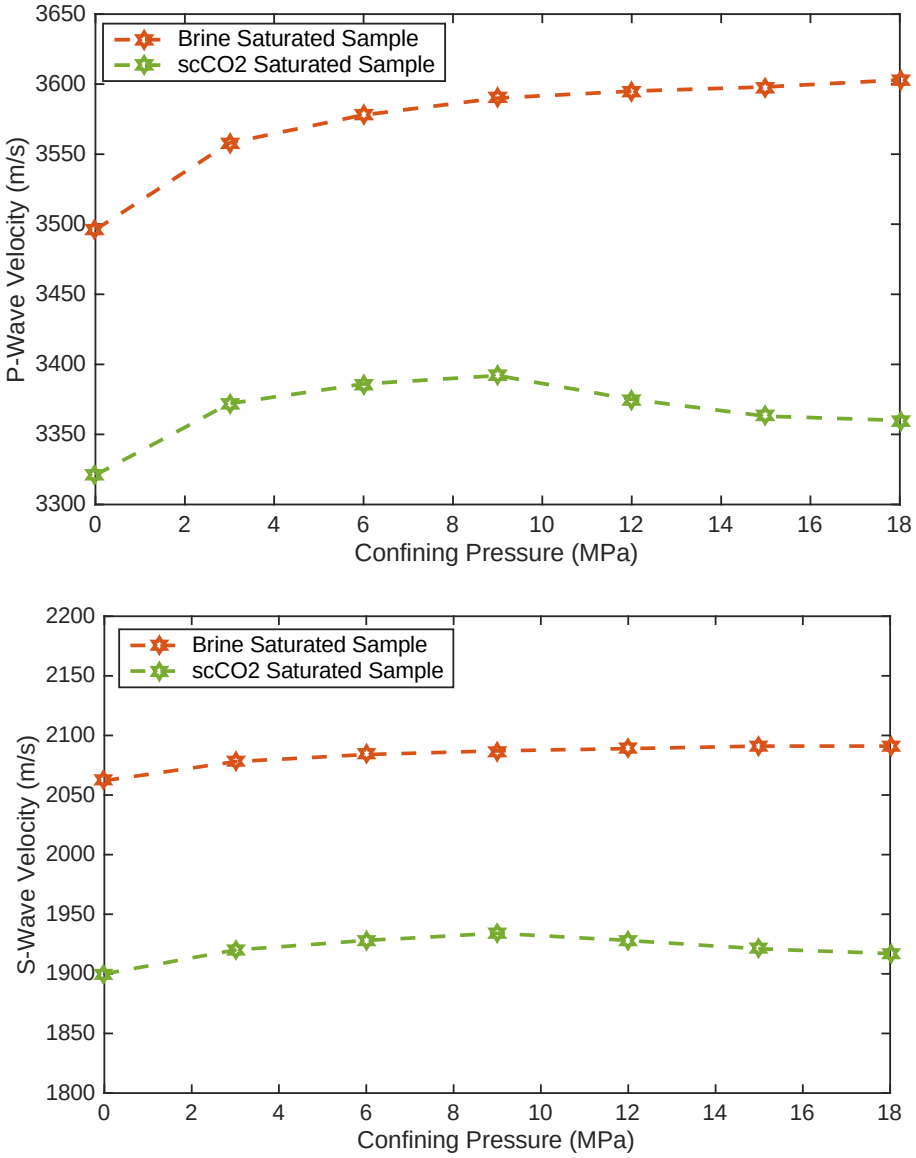

Figure 11: Compressional and shear wave velocities in the $scCO_2$ and brine saturated samples with respect to confining pressure under the differential pressure of 3MPa

As it is shown in this Figure, the brine-saturated sample gives a higher velocity of P-wave with a value up to 3600 m/s at the confining pressure of 18 MPa (i.e., the pore pressure of 15 MPa and a differential pressure of 3MPa) while the $scCO_2$-saturated sample shows a lower P-wave velocity which initially increases to 3390 m/s at the confining pressure of 9 MPa and then reduces constantly with a slow rate reaching 3350 m/s. The difference in velocities between the samples is especially manifest at the later stage when the confining and pore pressure increases.

The results obtained from the variation of the shear velocity, however, were not very easy to

interpret. In fact, looking at Figure 11, it seems that the shear velocity is sensitive to the fluid types in the pore space, which needs further investigations. The other interesting observation was the reduction of the shear velocity in the $scCO_2$ saturated sample after reaching the confining pressure of 9 MPa, which could be due to increases in the density of samples, alteration of the solid skeleton, or even pore pressure disequilibrium. This can be further evaluated by determination of dynamic shear modulus of the samples with different fluids substitutions.

It has been indicated by many that the strength of a rock can be decreased because of the fluid substitution in the pore space which might be related to mechanical actions of fluids or chemical interactions posed by pore fluids as the surface free energy reduced. However, there are very few studies reporting changes in mechanical responses of CO_2-saturated Berea sandstone. The study performed by Oikawa et al.(2008) and Hangx et al., (2013) suggested that the difference in the strength between the water saturated and the CO_2-saturated sandstone samples are very small. To further evaluate these changes, dynamic elastic parameters including Young's modulus, Poisson's ratio as well as shear modulus were estimated using the conventional equations provided by Mavko et al., (2009), assuming that the sample is homogenous and isotropic. The results obtained from this analysis on the dry sample were already reported in Table 4. Figures 12 shows the variation of the Young's and shear moduli obtained from this analysis.

Looking at this figure, one can conclude that the there is a reduction in the variation of elastic parameters especially the shear modulus. This indicates the fact that the decrees in the shear velocity was not only because of the increases in the density of the sample. It could also be due to mineralogical alterations and dissolution of calcite and break down of clays in the matrix after exposure to $scCO_2$ (Marbler et al., 2012). Generation of carbonic acid may be the other reason leading to the dissolution of carbonates including calcite and a long-term dissolution of feldspars, clay minerals, micas and Fe-oxides during and after injection. According to Marbler et al. (2012), dissolution of CO_2 into brine saturated sandstone samples changes its ability to resist against differential stresses. Le Guen et al. (2007) observed a clear strength reduction in the wet sandstone due to CO_2 injection.

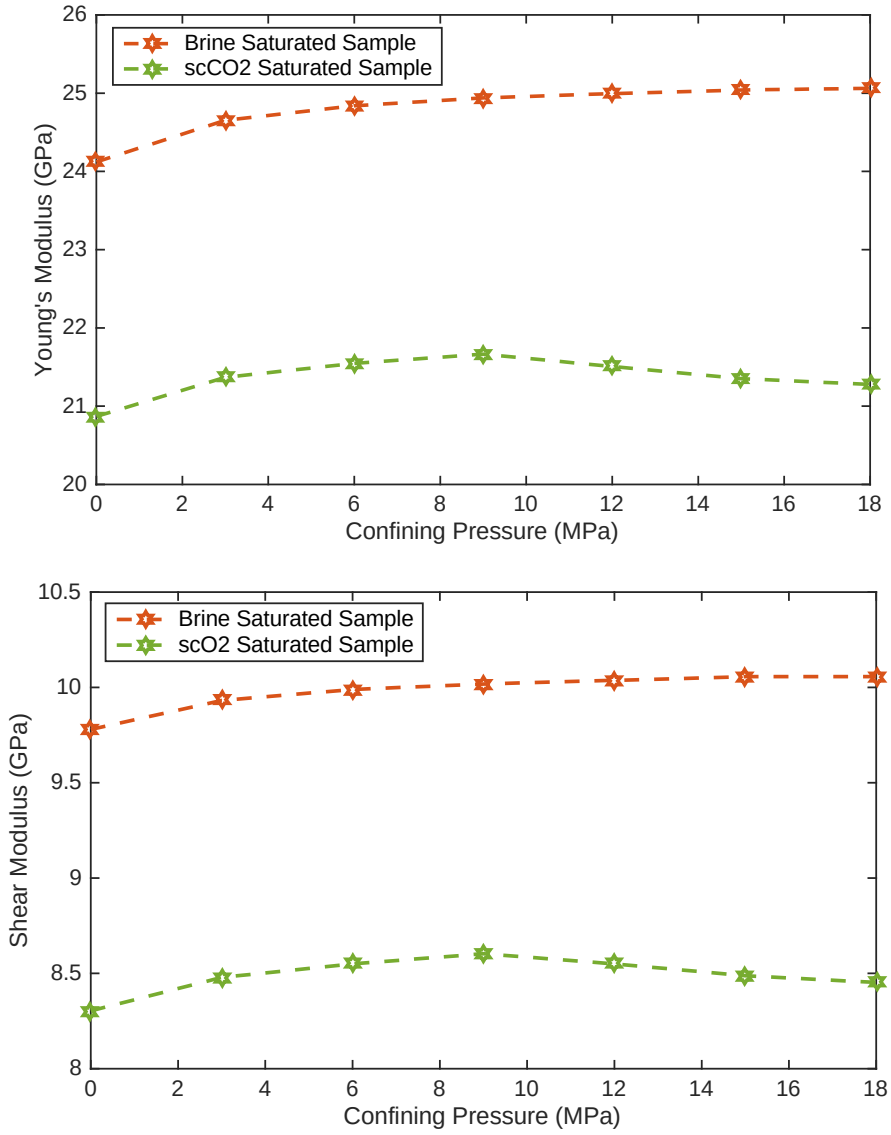

Figure 12: Variations of Young's and shear's Modulus in the $scCO_2$ and brine saturated samples with respect to confining pressure under the differential pressure of 3MPa

To further evaluate the alteration of the solid skeleton, the SEM images of the Berea sandstone before and after exposure to $scCO_2$ were studied as shown in Figure 13 and 14. Table 8 and 9 gives the element type, their weight concentrations and stoichiometric percentage[2] obtained from the same analysis before and after exposure to $scCO_2$.

The results obtained revealed that the alteration was induced and mineral dissolutions and corrosions were taken place, as shown in Figure 14. In fact, it seems that the main concerns are corrosion of quartz, K-feldspars and clay minerals (kaolinite) as well dissolution of carbonates

[2] - The percentage in which those elements were involved in the reactions taken place due to $scCO_2$ exposure

(calcite) (See Table 9). It should also be noticed that Kaolinites often gives marginal mineral dissolution as well whereas K-feldspar usually prevails surface solutions and its reaction with carbon dioxide in the aqueous solution of aquifer can results in the formation of bicarbonate, silica and kaolinite Holdren and Berner (1979).

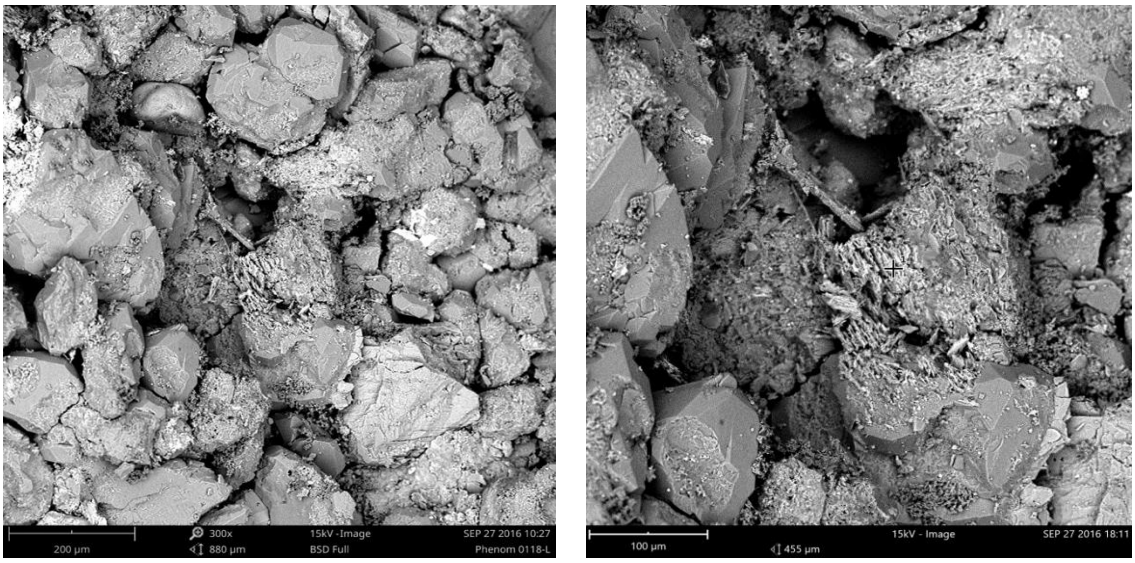

Figure 13: The Berea Sandstone before exposure to $scCO_2$

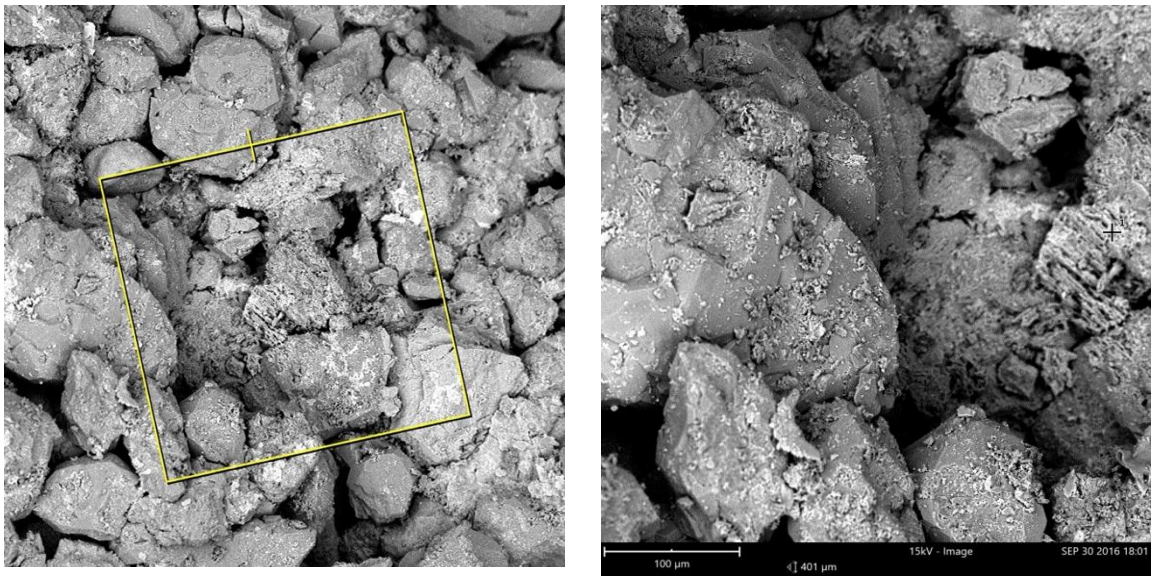

Figure 14: The Berea Sandstone after exposure to $scCO_2$ with signs of changes and alteration in the solid framework

The surface of the sandstone sample shows a clear alteration of the cement matrix, such as initial dissolution of calcite. This dissolution of the carbonate matrix which was observed after five days of the experiment could also be linked to the formation of HCO_3^- as mentioned earlier.

Small grains of secondary carbonate minerals were also observed on the surfaces of quartz in the SEM images (Figure 14 right). Some of quartz crystals demonstrate selective surface corrosions which may destabilize the microstructure of the sandstone, due to changes of porosity within the boundary between cement and grains.

Table 8: Element quantification before exposure to $scCO_2$

Element Symbol	Atomic Concentration	Weight Concentration	Stoichiometric Percentage
O	74.81	62.81	
Si	17.74	26.15	70.41
Al	5.42	7.68	21.52
K	1.00	2.05	3.96
Mg	1.03	1.32	4.10

Looking at Table 9, the concentration and percentage of certain elements may indicate the stage at which the primary minerals dissolve and secondary minerals precipitate in the solution. In this regard, the concentrations of Na, K, Ca, Mg, as well as Si and Al would be particularly important.

Table 9: Element quantification after exposure to $scCO_2$

Element Symbol	Atomic Concentration	Weight Concentration	Stoichiometric Percentage
O	71.61	57.92	
Si	17.95	25.48	63.23
Al	3.83	5.23	13.50
Cl	1.79	3.21	6.32
Ca	1.37	2.78	4.83
Na	1.64	1.91	5.79
Fe	0.60	1.69	2.11
Mg	0.79	0.97	2.77
K	0.41	0.81	1.45

3. Conclusion

It is generally known that the long-term storage of CO_2 in a geologic medium is affected by complicated chemical interactions causing acidification, mineral dissolution, and changes in the in-situ stress, which in turn may have negative impacts on the elastic and strength parameters of reservoirs and seals. Out of geomechanical challenges, CO_2 breaching through formation fractures, initiated due to pressure buildup and geochemical interactions due to exposure to $scCO_2$, are of the primary concerns. In this paper, attempts were made to evaluate the geochemical alteration taking place in the Berea sandstone in a short period of time when it is saturated by brine and $scCO_2$. The results obtained indicated that reductions in the shear velocity and modulus which might be attributed to the corrosion of clays and dissolution of calcite in the matrix. This was further evaluated by the SEM image analysis, where clear

alteration of the sandstone was observed. In fact, there were signs of carbonate dissolution, kaolinite break-down and even corrosion of quartz which indicates the fact that geomechanical parameters of reservoirs and seals can be affected even in a short term exposure to $scCO_2$.

Acknowledgment

The authors would like to acknowledge "Curtin University Sarawak Malaysia" to fund this research through the Curtin Sarawak Research Institute (CSRI) Flagship scheme under the grant number CSRI-6015.

References

Alemu, B. L., Aker, E., Soldal, M., Johnsen, Ø., Aagaard., P. 2013. Effect of sub-core scale heterogeneities on acoustic and electrical properties of a reservoir rock: a CO2 flooding experiment of brine saturated sandstone in a computed tomography scanner, Geophys Prospect, 2013, 61, 235–250

Alonso, J., Navarro, V. and Calvo, B., 2012. Flow path development in different CO_2 storage reservoir scenarios: A critical state approach. Engineering Geology, 127: 54-64.

Arts, R., Vandeweijer, V., Hofstee, C., Pluymaekers, M., Loeve, D., Kopp, A. and Plug, W., 2012. The feasibility of CO_2 storage in the depleted P18-4 gas field offshore the Netherlands (the ROAD project). International Journal of Greenhouse Gas Control, 11: S10-S20.

Ashraf, M., 2014. Geological storage of CO_2: Heterogeneity impact on the behavior of pressure. International Journal of Greenhouse Gas Control, 28: 356-368.

Bachu, S., 2003. Screening and ranking of sedimentary basins for sequestration of CO_2 in geological media in response to climate change. Environmental Geology, 44(3): 277-289.

Bachu, S., 2008. CO2 storage in geological media: role, means, status, and barriers to deployment. Progress in Energy and Combustion Science 34, 254–273.

Batzle, M., Wang, Z., 1992. Seismic properties of pore fluids. Geophysics 57, 1396–1408.

Bachu, S., W.D. Gunter and E.H. Perkins, 1994: Aquifer disposal of CO2 : hydrodynamic and mineral trapping, Energy Conversion and Management, 35(4), 269–279.

Benisch, K. and Bauer, S., 2013. Short- and long-term regional pressure build-up during CO2 injection and its applicability for site monitoring. International Journal of Greenhouse Gas Control, 19: 220-233.

Birkholzer, J.T., Zhou, Q., Cortis, A. and Finsterle, S., 2011. A Sensitivity Study on Regional Pressure Buildup from Large-Scale CO_2 Storage Projects. Energy Procedia, 4(0): 4371-4378.

Buscheck, T.A., Sun, Y., Hao, Y., Wolery, T.J., Bourcier, W.L., Tompson, A.F.B., Jones, E.D., Friedmann, S.J., Aines, R.D., 2011. Combining brine extraction, desalination, and residual-brine reinjection with CO_2 storage in saline formations:implications for pressure management, capacity, and risk mitigation. Energy Procedia 4, 4283–4290.

Buscheck, T.A., Friedmann, S.J., Sun, Y., Chen, M., Hao, Y., Wolery, T.J. and Aines, R.D., 2012. Active CO_2 reservoir management for CO_2 capture utilization and storage: An approach to improve CO_2 storage capacity and to reduce risk, Carbon Management Technology Conference. Carbon Management Technology Conference.

Campos, R., Barrios, I. and Lillo, J., 2015. Experimental injection: Study of physical changes in sandstone porous media using Hg porosimetry and 3D pore network models. Energy Reports, 1: 71-79.

Chadwick, A., Arts, R., Bernstone, C., May, F., Thibeau, S. and Zweigel, P., 2008. Best practice for the storage of CO2 in saline aquifers. British Geological Survey Occasional Publication, 14: 267.

Chen,H., Yang, s., Huan, K., Li, F., Huang, W., Zheng, A., Zhang, X. 2013. Experimental Study on Monitoring CO2 Sequestration by Conjoint Analysis of the P‑Wave Velocity and Amplitude, Environ Sci Technol, 47 (17) :10071-10077.

Chester, F.M., Chester, J.S., Kronenberg, A.K., Hajash, A., 2007. Subcritical creep compaction of quartz sand at diagenetic conditions: effects of water and grain size. Journal of Geophysical Research 112, B06203.

Chiaramonte, L., Zoback, M., Friedmann, J., Stamp, V. and Zahm, C., 2011. Fracture characterization and fluid flow simulation with geomechanical constraints for a CO2–EOR and sequestration project Teapot Dome Oil Field, Wyoming, USA. Energy Procedia, 4: 3973-3980.

Cook, J., Frederiksen, R.A., Hasbo, K., Green, S., Judzis, A., Martin, J.W., Suarez-Rivera, R., Herwanger, J., Hooyman, P. and Lee, D., 2007. Rocks matter: Ground truth in geomechanics. Ground truth in geomechanics. Oilfield Review, 19(3), 36-55.

Carcione, J.M., Picotti, S., Gei, D., Rossi, G., 2006. Physics and seismic modelling for monitoring CO2 storage. Pure Appl Geophys 163, 175–207.

Dempsey, D., Kelkar, S. and Pawar, R., 2014. Passive injection: A strategy for mitigating reservoir pressurization, induced seismicity and brine migration in geologic CO_2 storage. International Journal of Greenhouse Gas Control, 28(0): 96-113.

De Silva, G.P.D., Ranjith, P.G. and Perera, M.S.A., 2015. Geochemical aspects of CO2 sequestration in deep saline aquifers: A review. Fuel, 155: 128-143.

Dewers, T.A., Hajash, A., 1995. Rate laws for water-assisted compaction and stress induced water–rock interaction in sandstones. Journal of Geophysical Research 100, 13093–13112.

Dilmore, R.M., Allen, D.E., Jones, J.R.M., Hedges, S.W. and Soong, Y., 2008. Sequestration of dissolved CO_2 in the Oriskany formation. Environmental science & technology, 42(8): 2760-2766.

Doughty, C., 2010. Investigation of CO_2 plume behavior for a large-scale pilot test of geologic carbon storage in a saline formation. Transport in porous media, 82(1): 49-76.

Erickson, K.P., Lempp, C. and Pöllmann, H., 2015. Geochemical and geomechanical effects of scCO_2 and associated impurities on physical and petrophysical properties of Permotriassic Sandstones (Germany): an experimental approach. Environmental Earth Sciences, 74(6): 4719-4743.

Espinoza, D., Kim, S. and Santamarina, J., 2011a. CO_2 geological storage—geotechnical implications. KSCE Journal of Civil Engineering, 15(4): 707-719.

Evans, B., Saeedi, A., Rasouli, V., Liu, K. and Lebedev, M., 2012. Predicting CO_2 injectivity properties for application at CCS sites, Curtin University, Australia.

Feng, X. T., Chen, S., Zhou, H. 2004. Real-time computerized tomography (CT) experiments on sandstone damage evaluation during triaxial compression with chemical corrosion, Int. J. Rock Mech. Min. Sci. 41, 181–192.

Ferronato, M., Gambolati, G., Janna, C. and Teatini, P., 2010. Geomechanical issues of anthropogenic CO_2 sequestration in exploited gas fields. Energy Conversion and Management, 51(10): 1918-1928.

Fischer, S., Liebscher, A., Lucia, M. and Hecht, L., 2013. Reactivity of sandstone and siltstone samples from the Ketzin pilot CO_2 storage site-Laboratory experiments and reactive geochemical modeling. Environmental Earth Sciences, 70(8): 3687-3708.

Fischer, S., Zemke, K., Liebscher, A. and Wandrey, M., 2011. Petrophysical and petrochemical effects of long-term CO_2 -exposure experiments on brine-saturated reservoir sandstone. Energy Procedia, 4: 4487-4494.

Fjær, E., Holt, R., Horsrud, P., Raaen, A. and Risnes, R., 2008. Geological aspects of petroleum related rock mechanics. Developments in Petroleum Science, 53: 103-133.

Ghanbari, S., Al-Zaabi, Y., Pickup, G.E., Mackay, E., Gozalpour, F. and Todd, A.C., 2006. Simulation of CO_2 Storage In Saline Aquifers. Chemical Engineering Research and Design, 84(9): 764-775.

Goodarzi, S., Settari, A. and Keith, D., 2011. Geomechanical modeling for CO_2 storage in Wabamun Lake Area of Alberta, Canada. Energy Procedia, 4: 3399-3406.

Hangx, S., Spiers, C. and Peach, C., 2010. Creep of simulated reservoir sands and coupled chemical-mechanical effects of CO_2 injection. Journal of Geophysical Research: Solid Earth (1978–2012), 115(B9).

Hangx, S., van der Linden, A., Marcelis, F. and Bauer, A., 2013. The Effect of CO_2 on the mechanical properties of the Captain Sandstone: Geological Storage of CO_2 at the Goldeneye Field (UK). International Journal of Greenhouse Gas Control, 19(0): 609-619.

Hangx, S., Bakker, E., Bertier, P., Nover, G. and Busch, A., 2015. Chemical–mechanical coupling observed for depleted oil reservoirs subjected to long-term CO_2-exposure – A case study of the Werkendam natural CO_2 analogue field. Earth and Planetary Science Letters, 428: 230-242.

Hermanrud, C., Simmenes, T., Hansen, O.R., Eiken, O., Teige, G.M.G., Johansen, S., Bolaas, N., Marit, H. and Hansen, H., 2013. Importance of Pressure Management in CO_2 Storage, Offshore Technology Conference. Offshore Technology Conference.

Hildenbrand, A., Schlömer, S., Krooss, B. and Littke, R., 2004. Gas breakthrough experiments on pelitic rocks: comparative study with N2, CO2 and CH4. Geofluids, 4(1): 61-80.

Hitchon, B., ed., 1996. Aquifer Disposal of carbon dioxide: Hydrodynamic and mineral trapping – Proof of concept. Alberta: Geoscience Pulbishing. ISBN 0-9680844-0-0. 165 p.

Holdren GR Jr, Berner RA, 1979. Mechanism of feldspar weathering—I Experimental studies. Geochim Cosmochim Acta 43:1161–1171.

Huq, F., Haderlein, S.B., Cirpka, O.A., Nowak, M., Blum, P. and Grathwohl, P., 2015. Flow-through experiments on water–rock interactions in a sandstone caused by CO2 injection at pressures and temperatures mimicking reservoir conditions. Applied Geochemistry, 58: 136-146.

Hussain, F., Michael, K. and Cinar, Y., 2015. A numerical study of the effect of brine displaced from CO_2 storage in a saline formation on groundwater. Greenhouse Gases: Science and Technology.

Jung, Y., Zhou, Q. and Birkholzer, J.T., 2015. On the detection of leakage pathways in geological CO_2 storage systems using pressure monitoring data: Impact of model parameter uncertainties. Advances in Water Resources, 84: 112-124.

Kampman, N., Bickle, M., Wigley, M. and Dubacq, B., 2014. Fluid flow and CO_2–fluid–mineral interactions during CO_2-storage in sedimentary basins. Chemical Geology, 369(0): 22-50.

Karimnezhad, M., Jalalifar, H. and Kamari, M., 2014. Investigation of caprock integrity for CO_2 sequestration in an oil reservoir using a numerical method. Journal of Natural Gas Science and Engineering, 21: 1127-1137.

Kempka, T., De Lucia, M. and Kühn, M., 2014. Geomechanical integrity verification and mineral trapping quantification for the Ketzin CO_2 storage pilot site by coupled numerical simulations. Energy Procedia, 63: 3330-3338.

Kim, S. and Hosseini, S.A., 2014. Geological CO_2 storage: Incorporation of pore-pressure/stress coupling and thermal effects to determine maximum sustainable pressure limit. Energy Procedia, 63: 3339-3346.

Lebedev, M., Pervukhina, M., Mikhaltsevitch, V., Dance, T., Bilenko, O., and Gurevich, G 2013. An experimental study of acoustic responses on the injection of supercritical CO2 into sandstones from the Otway Basin. 78(4), D293-D306.

Le Guenan, T. and Rohmer, J., 2011. Corrective measures based on pressure control strategies for CO_2 geological storage in deep aquifers. international journal of Greenhouse Gas Control, 5(3): 571-578.

Le Guen, Y., Renard, F., Hellmann, R., Brosse, E., Collomber, M., Tisserand, D., Gratier, J.P. 2007. Enhanced deformation of limestone and sandstone in the presence of high PCO2 fluids, J. Geophys. Res. 112, 5421–5432.

Lynch, T., Fisher, Q., Angus, D. and Lorinczi, P., 2013. Investigating Stress Path Hysteresis in a CO_2 Injection Scenario using Coupled Geomechanical-Fluid Flow Modelling. Energy Procedia, 37: 3833-3841.

Madonna, C., Almqvist, B.S.G., Saenger, E.H., 2012. Digital rock physics: numerical prediction of pressure-dependent ultrasonic velocities using micro-CT imaging. Geophysical Journal International 189 (3), 1475–1482. http://dx.doi.org/ 10.1111/j.1365-246X.2012.05437.x.

Masoudi, R., Jalil, M., Press, D.J., Lee, K.-H., Phuat Tan, C., Anis, L., Darman, N.B. and Othman, M., 2011. An integrated reservoir simulation-geomechanical study on feasibility of CO_2 storage in M4 carbonate reservoir, Malaysia, International Petroleum Technology Conference. International Petroleum Technology Conference.

Marbler, H., Erickson, K. P., Schmidt, M., Lempp, C., Pollmann, H. 2012. Geomechanical and geochemical effects on sandstones caused by the reaction with supercritical CO2: an experimental approach to in situ conditions in deep geological reservoirs, Environ. Earth Sci. 69, 1981–1998.

Mbia, E.N., Frykman, P., Nielsen, C.M., Fabricius, I.L., Pickup, G.E. and Bernstone, C., 2014. Caprock compressibility and permeability and the consequences for pressure development in CO_2 storage sites. International Journal of Greenhouse Gas Control, 22(0): 139-153.

Meadows, M., 2008. Time-lapse seismic modeling and inversion of CO_2 saturation for storage and enhanced oil recovery. The Leading Edge 27 (4), 506–516.

Metz, B., Davidson, O., de Coninck, H., Loos, M., & Meyer, L. , 2005. IPCC, 2005: IPCC special report on carbon dioxide capture and storage. Prepared by Working Group III of the Intergovernmental Panel on Climate Change. Cambridge, United Kingdom and New York, NY, USA, 442 pp.

Njiekak, G., Schmitt, D.R., Yam, H., and Kofman, R. 2013, CO2 rock physics as part of the Weyburn-Midale geological storage, project: Int. J. Greenh Gas Con, DOI: 10.1016/j.ijggc.2013.02.007.

Noiriel, C., Gouze, P. and Madé, B., 2013. 3D analysis of geometry and flow changes in a limestone fracture during dissolution. Journal of hydrology, 486: 211-223.

Noiriel, C., Madé, B. and Gouze, P., 2007. Impact of coating development on the hydraulic and transport properties in argillaceous limestone fracture. Water resources research, 43(9).

Oikawa, Y., Takehara, T., Tosha, T., 2008. Effect of CO2 injection on mechanical properties of Berea sandstone. In: The 42nd U.S. Rock Mechanics Symposium(USRMS). American Rock Mechanics Association https://www.onepetro.org/conference-paper/ARMA-08-068.

Olden, P., Pickup, G., Jin, M., Mackay, E., Hamilton, S., Somerville, J. and Todd, A., 2012. Use of rock mechanics laboratory data in geomechanical modelling to increase confidence in CO_2 geological storage. International Journal of Greenhouse Gas Control, 11: 304-315.

Oruganti, Y., Gupta, A.K. and Bryant, S.L., 2011. Analytical estimation of risk due to pressure buildup during CO_2 injection in deep saline aquifers. Energy Procedia, 4: 4140-4147.

Pervukhina, M., B. Gurevich, D. N. Dewhurst, and A. F. Siggins, 2010, Applicability of velocity-stress relationships based on the dual porosity concept to isotropic porous rocks: Geophys J Int, 181, 1473–1479.

Ranganathan, P., Van, H.P., Rudolph, E., Susanne, J. Zitha PZJ, 2011, Numerical modeling of CO2 mineralisation during storage in deep saline aquifers, Energy 4, 4538–4545.

Rathnaweera, T.D., Ranjith, P.G., Perera, M.S.A., Haque, A., Lashin, A., Al Arifi, N., Chandrasekharam, D., Yang, S.Q., Xu, T., Wang, S.H. and Yasar, E., 2015. CO_2-induced mechanical behaviour of Hawkesbury sandstone in the Gosford basin: An experimental study. Materials Science and Engineering: A, 641: 123-137.

Rathnaweera, T.D., Ranjith, P.G. and Perera, M.S.A., 2016. Experimental investigation of geochemical and mineralogical effects of CO2 sequestration on flow characteristics of reservoir rock in deep saline aquifers. Scientific Reports, 6: 19362.

Raza, A., Rezaee, R., Bing, C.H., Gholami, R., Hamid, M.A. and Nagarajan, R., 2015a. Carbon dioxide storage in subsurface geologic medium: A review on capillary trapping mechanism. Egyptian Journal of Petroleum (EGYJP)-Elsevier (in press), will be published in vol. 25, 2016.

Raza, A., Rezaee, R., Gholami, R., Rasouli, V., Bing, C.H., Nagarajan, R. and Hamid, M.A., 2015b. Injectivity and quantification of capillary trapping for CO_2 storage: A review of influencing parameters. Journal of Natural Gas Science and Engineering, 26: 510-517.

Ravazzoli, C.L. and Gómez, J.L., 2011. AVA seismic reflectivity analysis in carbon dioxide accumulations: Sensitivity to CO_2 phase and saturation. Journal of Applied Geophysics, 73(2): 93-100.

Renard, F., Park, A., Ortoleva, P., Gratier, J.-P., 1999. An integrated model for transitional pressure solution in sandstones. Tectonophysics 312, 97–115.

Riaz, A. and Cinar, Y. Carbon dioxide sequestration in saline formations: Part I—Review of the modeling of solubility trapping. Journal of Petroleum Science and Engineering, 124: 367-380 (2014).

Rochelle, C., Bateman, K., Pearce, J.,, 2002. Geochemical interactions between supercritical CO_2 and the Utsira Formation: an experimental study. In: British Geological Survey Report CR/02/060: 57.

Rutqvist, J., Birkholzer, J., Cappa, F. and Tsang, C.F., 2007. Estimating maximum sustainable injection pressure during geological sequestration of CO_2 using coupled fluid flow and geomechanical fault-slip analysis. Energy Conversion and Management, 48(6): 1798-1807.

Rutqvist, J., Birkholzer, J.T. and Tsang, C.-F., 2008. Coupled reservoir–geomechanical analysis of the potential for tensile and shear failure associated with CO_2 injection in multilayered reservoir–caprock systems. International Journal of Rock Mechanics and Mining Sciences, 45(2): 132-143.

Shapiro, S. A., 2003, Elastic piezosensitivity of porous and fractured rocks: Geophysics, 68, no. 2, 482–486, doi: 10.1190/1.1567215.

Shi, J.-Q. and Durucan, S., 2009. A coupled reservoir-geomechanical simulation study of CO_2 storage in a nearly depleted natural gas reservoir. Energy Procedia, 1(1): 3039-3046.

Shi, J.-Q., Smith, J., Durucan, S. and Korre, A., 2013. A Coupled Reservoir Simulation-geomechanical modelling study of the CO_2 Injection-induced Ground Surface Uplift Observed at Krechba, in Salah. Energy Procedia, 37: 3719-3726.

Shukla, R., Ranjith, P., Haque, A. and Choi, X., 2010. A review of studies on CO_2 sequestration and caprock integrity. Fuel, 89(10): 2651-2664.

Shukla, R., Ranjith, P. G., Choi, S. K., Haque, A., Yellishetty, M., Hong, L. 2012. Mechanical behaviour of reservoir rock under brine saturation, Rock Mech. Rock Eng. 46 (1),83–89.

Schutt, H., Wigand, M., Spangenberg, E. 2005. Geophysical and geochemical effects of supercritical CO2 on sandstones, Int. J. Geophys. 2, 767–786.

Snippe, J. and Tucker, O., 2014. CO_2 fate comparison for depleted gas field and dipping saline aquifer. Energy Procedia, 63(0): 5586-5601.

Solomon, S., 2006. Criteria for intermediate storage of carbon dioxide in geological formations. The Bellona Foundation, Oslo.

Szulczewski, M.L., MacMinn, C.W. and Juanes, R., 2011. How pressure buildup and CO2 migration can both constrain storage capacity in deep saline aquifers. Energy Procedia, 4(0): 4889-4896.

Thakur, N., Rajput, S., 2010. Exploration of Gas Hydrates. Springer, Heidelberg, Germany; New York

Tian, H., Xu, T., Li, Y., Yang, Z. and Wang, F., 2015. Evolution of sealing efficiency for CO_2 geological storage due to mineral alteration within a hydrogeologically heterogeneous caprock. Applied Geochemistry, 63: 380-397.

Tillner, E., Shi, J.-Q., Bacci, G., Nielsen, C.M., Frykman, P., Dalhoff, F. and Kempka, T., 2014. Coupled dynamic flow and geomechanical simulations for an integrated assessment of CO_2 storage impacts in a saline aquifer. Energy Procedia, 63: 2879-2893.

Ukaegbu, C., Gundogan, O., Mackay, E., Pickup, G., Todd, A. and Gozalpour, F., 2009. Simulation of CO_2 storage in a heterogeneous aquifer. Proceedings of the Institution of Mechanical Engineers, 223(A3): 249-267.

Varre, S.B.K., Siriwardane, H.J., Gondle, R.K., Bromhal, G.S., Chandrasekar, V. and Sams, N., 2015. Influence of geochemical processes on the geomechanical response of the overburden due to CO_2 storage in saline aquifers. International Journal of Greenhouse Gas Control, 42: 138-156.

Vidal-Gilbert, S., Tenthorey, E., Dewhurst, D., Ennis-King, J., Van Ruth, P. and Hillis, R., 2010. Geomechanical analysis of the Naylor Field, Otway Basin, Australia: Implications for CO_2 injection and storage. International Journal of Greenhouse Gas Control, 4(5): 827-839.

Vulin, D., Kurevija, T. and Kolenkovic, I., 2012. The effect of mechanical rock properties on CO_2 storage capacity. Energy, 45(1): 512-518.

Wainwright, H.M., Finsterle, S., Zhou, Q. and Birkholzer, J.T., 2013. Modeling the performance of large-scale CO2 storage systems: A comparison of different sensitivity analysis methods. International Journal of Greenhouse Gas Control, 17: 189-205.

Varre, S.B.K., Siriwardane, H.J., Gondle, R.K., Bromhal, G.S., Chandrasekar, V. and Sams, N., 2015. Influence of geochemical processes on the geomechanical response of the overburden due to CO_2 storage in saline aquifers. International Journal of Greenhouse Gas Control, 42: 138-156.

Zemke, K., Liebscher, A. and Wandrey, M., 2010. Petrophysical analysis to investigate the effects of carbon dioxide storage in a subsurface saline aquifer at Ketzin, Germany (CO_2 SINK). International Journal of Greenhouse Gas Control, 4(6): 990-999.

Zhang, Y., Langhi, L., Schaubs, P.M., Piane, C.D., Dewhurst, D.N., Stalker, L. and Michael, K., 2015. Geomechanical stability of CO_2 containment at the South West Hub Western Australia: A coupled geomechanical–fluid flow modelling approach. International Journal of Greenhouse Gas Control, 37: 12-23.

Zhu, Q., Zuo, D., Zhang, S., Zhang, Y., Wang, Y. and Wang, L., 2015. Simulation of geomechanical responses of reservoirs induced by CO_2 multilayer injection in the Shenhua CCS project, China. International Journal of Greenhouse Gas Control, 42: 405-414.